Gut and Liver
https://doi.org/10.5009/gnl240302
pISSN 1976-2283 eISSN 2005-1212

Review Article

Advanced Imaging Techniques for Assessing Fat, Iron, and Fibrosis in Chronic Liver Disease

Sabarish Narayanasamy[1], Manuela Franca[2], Ilkay S. Idilman[3], Meng Yin[1], Sudhakar K. Venkatesh[1]

[1]Department of Radiology, Mayo Clinic, Rochester, MN, USA; [2]Department of Radiology, Santo António University Hospital Centre, School of Medicine and Biomedical Sciences (ICBAS), University of Porto, Porto, Portugal; [3]Department of Radiology, Liver Imaging Team, Hacettepe University, Ankara, Turkiye

Article Info
Received June 30, 2024
Revised August 4, 2024
Accepted August 8, 2024
Published online January 8, 2025

Corresponding Author
Sudhakar K. Venkatesh
ORCID https://orcid.org/0000-0002-7514-1030
E-mail venkatesh.sudhakar@mayo.edu

Imaging plays a critical role in the management of chronic liver disease (CLD) because it is a safe and painless method to assess liver health. The widely used imaging techniques include ultrasound, computed tomography and magnetic resonance imaging. These techniques allow the measurement of fat deposition, iron content, and fibrosis, replacing invasive liver biopsies in many cases. Early detection and treatment of fibrosis are crucial, as the disease can be reversed in its early stages. Imaging also aids in guiding treatment decisions and monitoring disease progression. In this review, we describe the most common imaging manifestations of liver disease and the current state-of-the-art imaging techniques for the evaluation of liver fat, iron, and fibrosis. **(Gut Liver 2025;19:31-42)**

Key Words: Chronic liver disease; Steatosis; Iron overload; Liver fibrosis; Steatohepatitis

INTRODUCTION

Chronic liver disease (CLD) is a growing global health concern with metabolic dysfunction-associated steatotic liver disease (MASLD) emerging as the most prevalent etiology.[1] MASLD ranges from simple hepatic steatosis to more severe forms involving inflammation and hepatocellular injury or ballooning (metabolic dysfunction-associated steatohepatitis, MASH) and can progress to fibrosis and cirrhosis if untreated.[2] MASLD is intricately linked with metabolic syndrome and cardiovascular disease, constituting a major cause of morbidity and mortality worldwide.[3] Imaging plays a pivotal role in the evaluation and management of CLDs, offering noninvasive techniques to assess liver fat deposition, liver iron content, and liver fibrosis. These noninvasive quantitative imaging biomarkers for liver disease have replaced liver biopsy as the investigation of choice in many clinical settings. Early detection and treatment of fibrosis are key to improving survival rates, as fibrosis in its early stages is reversible.[4] Additionally, imaging serves as a valuable tool for guiding therapeutic strategies and monitoring disease progression in patients with CLD. Table 1 presents some of the most common etiologies of CLD. This review will delve into the various imaging techniques used in the assessment of CLD–ultrasound (US), computed tomography (CT), and magnetic resonance imaging (MRI).

Table 1. Common Causes of Chronic Liver Disease

Metabolic dysfunction-associated steatotic liver disease
Alcoholic liver disease
Hepatitis B
Hepatitis C
Autoimmune hepatitis
Hemochromatosis
Wilson disease
Primary biliary cholangitis
Primary sclerosing cholangitis
Drug-induced liver injury
Budd-Chiari syndrome
Idiopathic/cryptogenic

IMAGING OF HEPATIC STEATOSIS

Hepatic steatosis is histologically defined by the presence of fat droplets in more than 5% of the hepatocytes. It is the hallmark of MASLD, but it can be frequently encountered on imaging with other CLDs, such as alcohol-associated liver disease, viral hepatitis and genetic disorders. MASLD is the most common cause of CLD worldwide and a huge global problem.[1] MASLD includes a spectrum of conditions ranging from hepatic steatosis on one end to inflammation (steatohepatitis) and cirrhosis at the other end. Around 20% of the patients with hepatic steatosis will develop MASH and 20% of the patients with MASH may progress to fibrosis and cirrhosis.[5] Moreover, MASLD is closely linked to metabolic syndrome and cardiovascular disease, with cardiovascular events being the primary cause of mortality in these patients rather than liver-related complications.[3]

Traditionally, liver biopsy was considered the gold standard for assessing liver fat.[6] However, biopsy has significant drawbacks, including limited repeatability, risk of bleeding, pain, and sampling errors. Therefore, noninvasive imaging techniques have now replaced biopsy for detection of hepatic steatosis.

ULTRASOUND

US is the most commonly used imaging technique to evaluate patients with suspected hepatic steatosis. On US, hepatic steatosis appears as increased liver echogenicity or a "bright" liver (Fig. 1). US can also be used to grade steatosis as mild (slight increased echogenicity), moderate (increased echogenicity with blurring of adjacent portal vessels) and severe (additional blurring of the diaphragm).[7] A major advantage of US is wide availability and low cost. Importantly, coexisting liver iron does not influence fat estimation on US, unlike CT and MRI.[8] However, US is highly operator dependent, it is insensitive in cases of mild steatosis and its performance is affected by liver fibrosis, which also increases the liver echogenicity. US may also be limited in the presence of ascites or in obese patients. However, newly developed quantitative US techniques use parameters such as the attenuation coefficient and backscatter coefficient to provide objective measurements of hepatic steatosis, which helps mitigate subjectivity and operator-dependency associated with conventional US.[9]

COMPUTED TOMOGRAPHY

CT can also be used to assess liver fat content, although it is less sensitive than MRI. Fatty liver demonstrates low attenuation on CT represented by a decrease in Hounsfield units (HU). Typically, a normal liver shows attenuation values of around 65 to 70 HU on unenhanced CT and appears denser than the spleen.[10] However, with increasing steatosis, the liver becomes hypodense (darker) than the fat-free spleen. Unenhanced CT has been shown to be sensitive and specific in detection moderate to severe steatosis when a cutoff value of 48 HU is used (Fig. 2).[11] Recently, studies have demonstrated a linear relationship between HU values measured on unenhanced CT and proton density fat fraction (PDFF) measured on MRI.[10] It is important to remember that measurements on contrast CT are less accurate, as the contrast increases the liver attenuation values. Abdominal CT is very commonly performed in the United States for various indications, offering a chance for opportunistic screening of MASLD. Conditions that alter liver attenuation, such as iron overload, certain medications like amiodarone, inflammation and advanced fibrosis and cirrhosis may also interfere with fat estimation. Dual-energy CT, at present remains only an investigational technique in this context and does not offer any additional benefit over conventional CT due to the similar attenuation coefficients of fat and iron.

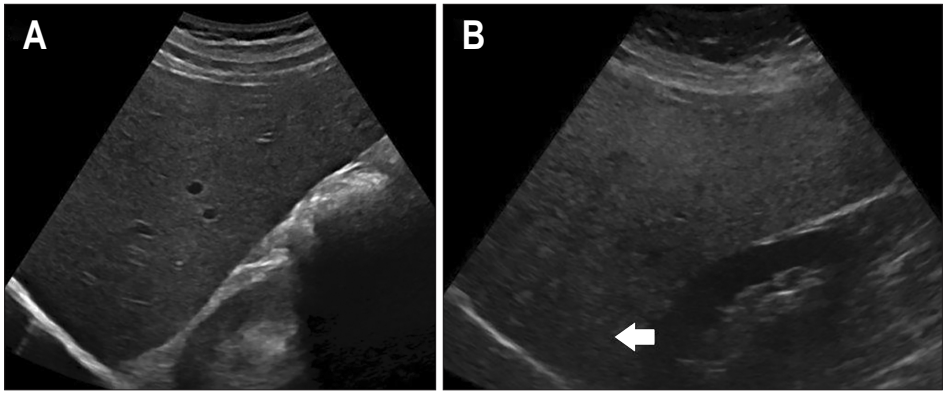

Fig. 1. Hepatic steatosis on ultrasound (US). B-mode transverse US images of a normal liver (A) and a steatotic liver (B). A steatotic liver is diffusely echogenic with attenuation of the deeper parts of the liver.

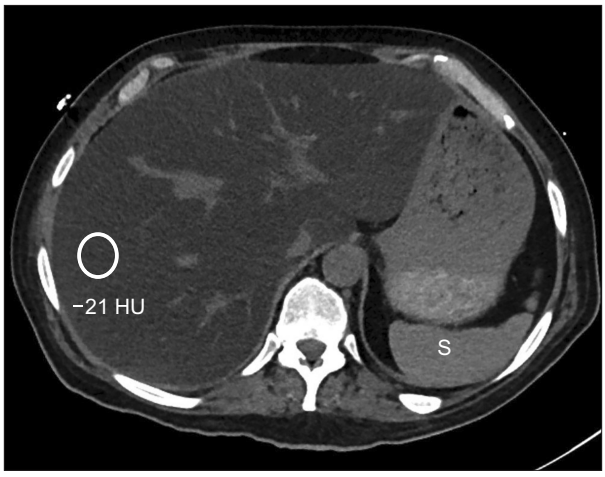

Fig. 2. Severe hepatic steatosis on computed tomography (CT). Axial non-contrast enhanced CT shows diffuse hypoattenuation of the liver parenchyma. The mean Hounsfield unit (HU) is −21 HU, which is consistent with severe steatosis. Note the spleen (S) is hyperdense compared to the liver

MAGNETIC RESONANCE IMAGING

MRI is currently the preferred modality for assessing hepatic steatosis.[12] Conventional in-phase and out-of-phase imaging (dual echo chemical shift imaging) can be used to qualitatively detect liver steatosis. In this technique, a fatty liver demonstrates diffuse signal loss on out-of-phase images compared to the in-phase images due to differences in precession frequencies of fat and water protons. This method enables a qualitative assessment (signal intensity ratio, SIR) of steatosis as mild, moderate, and severe. However, this SIR is a semi-quantitative assessment of hepatic steatosis and can be affected by several technical factors and corrections applied to the sequence by different MR vendors. Quantitative measurement of liver fat can be achieved using MR spectroscopy (MRS) or chemical shift encoded (CSE) imaging.

1. MR spectroscopy

MRS works by exploiting the distinct magnetic resonance frequencies of water and fat molecules within the liver.[13] By analyzing the spectral peaks associated with fat and water, MRS can precisely quantify the relative fat content within the liver parenchyma. It was one of the earliest methods used to assess liver fat using MRI. Although MRS is regarded as the gold standard for research and clinical trials, it is impractical for routine clinical use due to its complexity, time of acquisition and need for MR physics expertise. Moreover, MRS calculates fat signals within a single voxel, which can impact test repeatability and presents limitations like biopsy in terms of sampling variability.

2. CSE MRI

PDFF measured using CSE MRI is currently considered to be the most accurate and reliable method to measure liver fat.[12] PDFF represents the ratio of the signal in the liver due to fat molecules to the total signal in the liver. CSE MRI technique involves acquiring images at 3 or more echo times and then separating the fat and water signals. This is different from conventional in- and out-of-phase imaging which is a 2-point DIXON technique. This usually can be performed within a single breath hold. There are two major approaches to CSE MRI: magnitude-based and complex-based strategies. The magnitude-based strategy is generally easier to perform but is limited by low signal to noise ratio and a limited PDFF range. In contrast, complex-based strategies incorporate both the magnitude and the phase data and offer a much wider range of PDFF. The acquisition of multiple echoes allows for simultaneous estimation of PDFF and T2* decay rate (R2*), which is related with liver iron content. This confounder-corrected CSE MRI accounts for presence of coexisting liver iron and, therefore, can simultaneously calculate the PDFF and liver iron concentration (LIC) by measuring the liver R2*, enabling the creation of fat-free R2* maps and thus removing the confounding effect of hepatic iron on fat estimation and vice versa (Fig. 3). One study showed that PDFF estimates calculated using CSE MRI are unreliable above a R2* values of 538 s^{-1} at 1.5T and 779 s^{-1} at 3T.[14]

CSE MRI calculated PDFF demonstrates a very high intra-reader and inter-reader correlation and correlates strongly with histopathology.[15] It has been validated in multiple studies and is currently considered the ideal method for both the initial assessment of liver fat and monitoring response to treatment. Most of the MRI vendors provide commercial CSE packages to calculate PDFF and liver iron simultaneously. The entire protocol can be typically completed in less than 5 minutes of scan time and can be performed on both 1.5T and 3T scanners.[16] In our institution, this is combined with MR elastography (MRE) to form a rapid hepatogram protocol. Table 2 outlines the advantages and limitations associated with each technique.

IMAGING OF HEPATIC IRON DEPOSITION

Iron deposition in the liver may be seen in the setting of primary hemochromatosis or hemosiderosis.[17] Primary hemochromatosis is an autosomal recessive genetic disorder characterized by increased iron absorption and deposition in liver, pancreas, and the heart. Hemosiderosis, also referred to as secondary hemochromatosis, is most commonly due to repeated iron transfusions. This disorder is

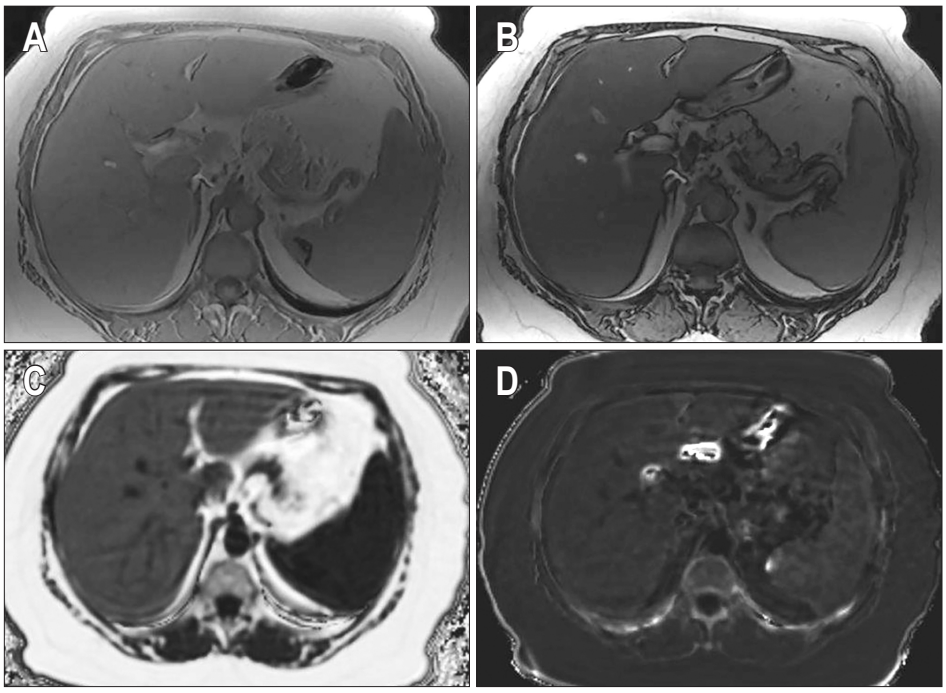

Fig. 3. Chemical shift encoded magnetic resonance images of a patient with severe hepatic steatosis. In-phase (A) and out-of-phase (B) images show diffuse loss of signal in the liver on out-of-phase image compared to the in-phase image, which is consistent with hepatic steatosis. Corrected proton density fat fraction (PDFF) (C) and R2* maps (D) are also shown at the bottom. The patient had a mean PDFF of 20%.

Table 2. Assessment of Hepatic Steatosis

Modality	Technique and imaging findings	Advantages	Limitations
Conventional ultrasound	Fatty liver shows increased liver echogenicity Grading into mild, moderate, and severe steatosis based on blurring of adjacent structures Hepatorenal index=hepatic SI intensity/renal cortex SI	Low cost Widely available Noninvasive Can be used for screening	Highly operator dependent Confounded by changing technical parameters Not useful for mild steatosis
Quantitative ultrasound	Attenuation coefficient Backscatter coefficient Speckle statistics	Quantitative Not operator dependent	Not widely available Needs validation
CT	Fatty liver demonstrates hypoattenuation on CT HU values on CT correlate with PDFF on MR PDFF (%) = −0.58× (HU) + 38.2	Easy to perform Widely available	Inaccurate for mild steatosis
MR spectroscopy	PRESS or STEAM Fat content in a single voxel is measured in right lobe Gold standard especially in clinical trials	Precise	Sampling variability Technically demanding Need for MR physicist Time consuming
MRI-PDFF	Most accurate method Chemical shift encoded MRI Can be combined with iron quantification	Accurate and fast Easily added to liver MRI Larger region of interest	Coexisting iron can be a confounder and should be corrected

SI, signal intensity; CT, computed tomography; HU, Hounsfield unit; PDFF, proton density fat fraction; MR, magnetic resonance; PRESS, point resolved spectroscopy; STEAM, stimulated echo acquisition mode; MRI, magnetic resonance imaging.

characterized by iron deposition in the reticuloendothelial system (liver, spleen, kidneys, and bone marrow).

Excess free iron regardless of the etiology can be cytotoxic, generating oxidative free radicals and causing cellular damage. Liver iron accumulation can lead to fibrosis and eventually cirrhosis. This is often clinically silent but can be diagnosed on imaging. Furthermore, hepatic iron overload can also be found in many other CLD, such as viral hepatitis, alcoholic hepatitis, MASLD, or dysmetabolic iron overload syndrome. Dysmetabolic iron overload syndrome refers to patients with hyperferritinemia-associated metabolic dysfunction and it has been considered within the same spectrum of disease as MASLD. In these patients, iron accumulates predominantly in the mononuclear phagocytic system (liver Kupffer cells and spleen), but rarely the amount of iron overload is as high as in hereditary hemochromatosis or transfusional hemosiderosis.[18]

Traditionally, serum ferritin level was used to estimate iron stores, but its reliability is limited by its role as acute phase reactant, which can be elevated in inflammatory

conditions. The liver is the primary site of iron storage in the body, and LIC correlates closely with total body iron stores.[19] Liver biopsy, once considered the gold standard for measuring LIC, is fraught with disadvantages including invasiveness, sampling variability, and associated risks of pain, bleeding, and complications. Consequently, MRI has emerged as the preferred method for LIC measurement, offering a noninvasive approach for follow-up and treatment response assessment without the need for repeat biopsies.[17] Long-term annual liver iron quantification with MR is recommended for patients undergoing repeated blood transfusions.

1. Computed tomography

CT can be used to detect iron overload, albeit with a lower sensitivity than MRI. The liver usually shows a uniform increase in attenuation above 70 to 75 HU with iron overload (Fig. 4).[20] However, it is important to note that certain drugs like amiodarone, gold, copper deposition in Wilson disease, and glycogen storage diseases can also elevate liver attenuation. Additionally, the presence of coexisting hepatic steatosis can reduce the sensitivity of CT for detecting liver iron due to decreased attenuation.

Fig. 4. Hepatic iron overload on computed tomography (CT) images. Non-contrast enhanced CT image of the liver shows diffuse increased attenuation of the liver and spleen in a patient with iron overload secondary to repeated blood transfusions. HU, Hounsfield unit.

2. Magnetic resonance imaging

Iron deposition leads to shortening of T1, T2, and T2* relaxation times, along with an increase in the R2* relaxation rate. On conventional imaging sequences, it is often possible to suggest a diagnosis of iron overload by comparing dual gradient in-phase and out-of-phase sequences. Iron deposition results in a signal drop in the affected organs on in-phase (second-echo) images compared to the out-of-phase (first echo) images. This occurs because of the paramagnetic effect of iron, which increases the signal decay, that will be greater on images acquired at a longer echo time (in-phase images) compared to out-of-phase images, which are acquired with the shortest echo time. This is in direct contrast to hepatic steatosis, where there is a loss of signal on the out-of-phase images. Additionally, the iron-overloaded liver also demonstrates decreased signal intensity (SI) compared to the spleen on conventional T2 fast spin echo images.[21]

It is important to note that as the liver SI can be affected by both fat and iron, these conventional MRI sequences will not be reliable for diagnosing steatosis or iron overload, if fat and iron coexist in the liver parenchyma, which is quite common in CLD.

3. Iron quantification by MRI

Quantitative assessment of LIC by MRI is as accurate as a biopsy in diagnosing iron overload. Numerous methods

Table 3. Assessment of Liver Iron

Modality	Technique and imaging findings	Advantages	Limitations
CT	Uniform hyperattenuation on CT HU >70 HU Qualitative assessment only	Easy to perform Widely available	Confounded by coexisting fat, drugs, (e.g., gold, amiodarone) or storage disorders
MRI-SIR	SIR between the liver and muscle Semi-quantitative assessment	Simple and easy to use Excellent correlation with biopsy	Limited dynamic range, Overestimates mild steatosis
MRI-R2 relaxometry (FerriScan*)	Based on single spin echo acquisitions Data is submitted to Resonance Health for image processing and centralized analysis	Wider range Approved in many countries	Long scan times Waiting time (2-day report turnaround time) Additional cost for analysis
MRI-R2* relaxometry	Most accurate method Based on CSE MRI–multiple gradient echo acquisitions Liver fat can be simultaneously measured	Widely validated on 1.5T and 3T Linear relationship with histology Low cost Faster acquisition	Limited at high liver iron concentration

CT, computed tomography; HU, Hounsfield unit; MRI, magnetic resonance imaging; SIR, signal intensity ratio; CSE, chemical shift encoded.

have been described for quantification including SIR techniques and T2*/R2* relaxometry techniques (Table 3).[22]

4. SIR technique

The SIR technique, pioneered by Gandon and colleagues, is a GRE (gradient echo)-based approach that compares liver SI with a reference organ unaffected by iron overload, such as the paraspinal muscle.[19] Normally, liver SI should be higher than that of muscle. With increasing iron deposition, liver signal diminishes, resulting in a darker appearance compared to muscle. A semi-quantitative assessment can be made by drawing regions of interest (ROI) on the liver and the paraspinal muscles and calculating the SIRs. However, this technique tends to overestimate mild to moderate iron overload, may not be reproducible across different vendors and has been surpassed by more advanced methods as discussed below.[23]

5. R2* relaxometry techniques

Iron deposition leads to magnetic field inhomogeneity, resulting in shortening of T2* times. R2* or the rate of relaxation is inversely proportional to T2* (1/T2*). Studies have shown that R2* values have a linear relationship with LIC content.[22,24] R2* relaxometry techniques utilize multi-echo GRE acquisitions with multiple TEs. Then, R2* parametric map is generated from which the R2* can be calculated. R2* values are measured by drawing multiple ROIs on the liver and a mean value is reported. R2* techniques can be performed at either 1.5T or 3T magnets, but 3T R2* measurements are the double of 1.5T R2* values.[25] The presence of co-existent liver fat can interfere with iron quantification and must be corrected, using the multi-echo CSE sequences described above. Thus, confounder-corrected quantitative CSE MRI using R2* relaxometry technique is currently the preferred method to simultane-

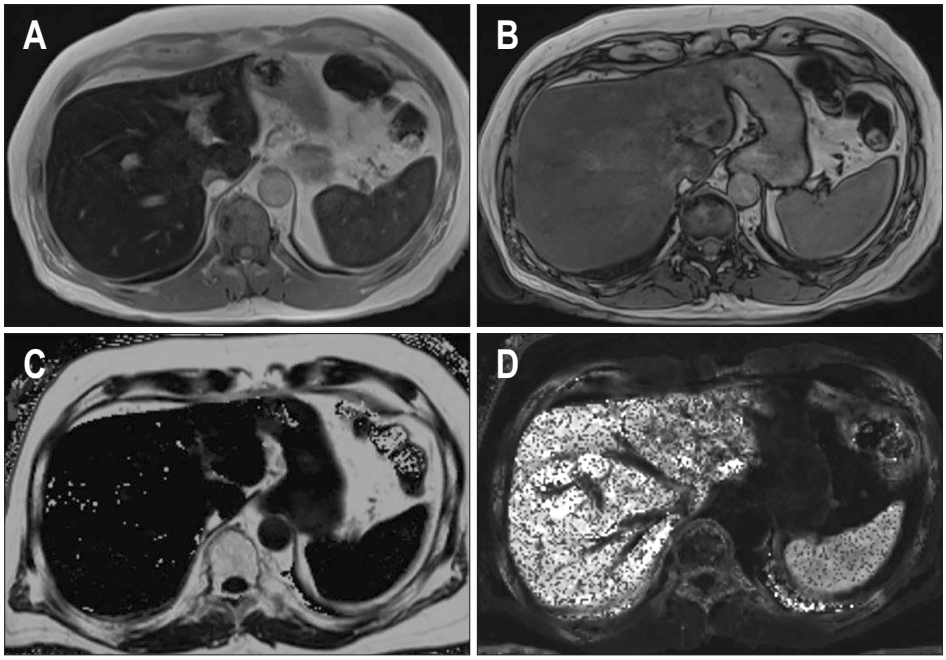

Fig. 5. Chemical shift encoded magnetic resonance images of a patient with hemosiderosis and severe iron overload in the liver and spleen. In-phase (A) and out-of-phase (B) images show loss of signal in the liver on in-phase images compared to the out-of-phase images suggesting iron overload. Corrected proton density fat fraction (C) and R2* maps (D) are shown at the bottom. Increased pixel intensity on the R2* map suggests iron overload. The patient had a mean R2* value of 683 s^{-1} equivalent to liver iron concentration of 9.91 mg Fe/g.

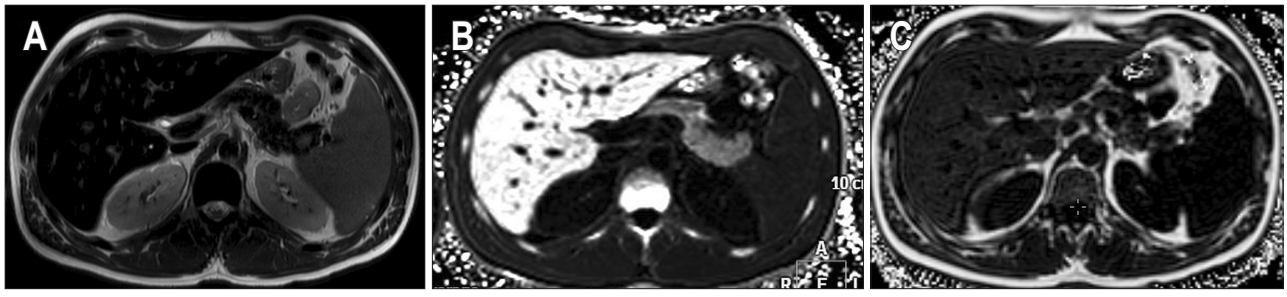

Fig. 6. Chemical shift encoded magnetic resonance images of a patient with hereditary hemochromatosis and severe iron overload in the liver and pancreas. T2-weighted (A), R2* map (B) and proton density fat fraction (PDFF) maps (C) are shown. There is low signal intensity of the liver and pancreas on T2 images due to iron deposition and normal signal intensity of the spleen. On the R2* map, the liver and pancreatic R2* are elevated (435 s^{-1} and 190 s^{-1}, respectively) and the spleen R2* is normal (50 s^{-1}). Mild hepatic steatosis was also observed on PDFF images (~9%).

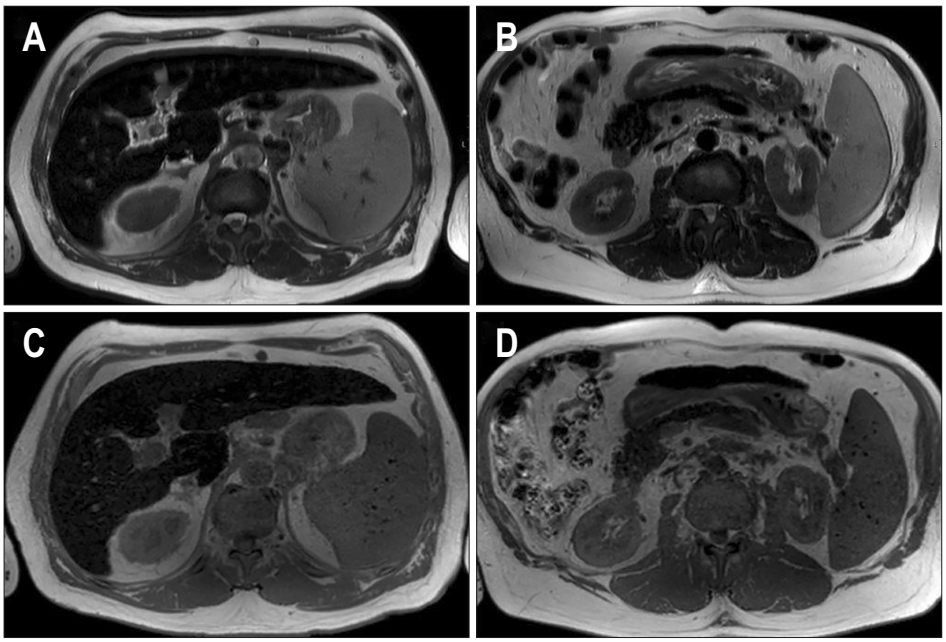

Fig. 7. Axial T2-weighted images (A, B) and axial T1 in-phase (C, D) images of a male patient with cirrhosis, hyperferritinemia (3,000 ng/mL) and elevated transferrin saturation (80%). There is low signal intensity of the liver and pancreas related to iron deposition. Hereditary hemochromatosis (HH) was excluded on the basis of negative genetic tests. Using a multi-echo sequence (not shown), the liver R2* was 735 s^{-1} (LIC 178 μmol/g), pancreatic R2* was 400 s^{-1} and spleen R2* was 40 s^{-1}. Although liver and pancreas involvement typically accomanies HH, patients with non-HH cirrhosis can also present iron overload in other organs, such as the pancreas mimicking HH.

ously quantify both fat and iron in the liver (Figs 5-7). This method produces fat-free R2* maps and enables simultaneous evaluation for both liver fat (PDFF) and iron (R2*). It has received regulatory approval and is widely available with all major MRI vendors.

IMAGING OF LIVER FIBROSIS AND CIRRHOSIS

Liver fibrosis and cirrhosis represent the end stage of CLD regardless of the underlying cause and are significant contributors to global mortality and morbidity. Early fibrosis is potentially reversible, underscoring the importance of early detection through imaging to initiate timely treatment and prevent progression to cirrhosis. Liver biopsy has historically been regarded as the reference standard for staging liver fibrosis but there has been a shift towards developing noninvasive imaging techniques (Table 4).

1. Ultrasound

US imaging plays a crucial role in the evaluation of CLD owing to its wide availability, noninvasiveness, and ability to provide valuable information about liver morphology and vascularization. In CLD, the US can detect liver parenchymal changes such as hepatomegaly, nodularity, and signs of cirrhosis. Morphologic changes of cirrhosis including caudate and left lobe hypertrophy, right lobe atrophy, nodularity of the liver surface and widening of the portal fissures have been well described on US. Additionally, the US is valuable for detecting complications such as ascites, portal hypertension, and for screening of hepatocellular carcinoma (HCC). Current guidelines recommend US screening every 6 months for HCC in high-risk patients.[26]

US elastography offers a noninvasive method to assess liver stiffness as an indicator of fibrosis. The two primary techniques of US elastography are vibration-controlled transient elastography and shear wave elastography. A comprehensive discussion of US elastography is beyond the scope of this article and can be found in other sources.[27]

2. Conventional MRI and CT

Cirrhosis is characterized by simultaneous fibrosis and regeneration resulting in coarse and nodular liver parenchyma. Historically, several morphological criteria have been described for diagnosing cirrhosis on MRI and CT, including irregular margins, modified caudate-right lobe ratio, enlargement of the hilar space, posterior notch sign and expansion of the gallbladder fossa (Fig. 8).[28,29] Of these features, widening of periportal space has been described to have high sensitivity for hepatic fibrosis.[30] MRI has a superior soft tissue resolution to CT and is an important technique in assessing patients with CLD. While morphological changes of cirrhosis are well depicted on conventional cross-sectional imaging, it is still limited in the evaluation of early hepatic fibrosis. Furthermore, advanced liver fibrosis may be present when morphology is normal. Conventional MRI and CT can also detect signs of portal hypertension such as splenomegaly, ascites, and collaterals and aid detection of HCC in patients with cirrhosis.

Table 4. Assessment of Liver Fibrosis and Cirrhosis

Modality	Technique and Imaging findings	Advantages and limitations	Limitations
Conventional CT and MRI	Surface nodularity Fissural widening Lobar and segmental volume changes-caudate to right lobe ratio, etc.	Easy to perform Simultaneously assess for HCC and portal hypertension	Poor detection of early fibrosis Not useful for treatment monitoring
VCTE or FibroScan	One dimensional technique A-mode images are used to guide transducer placement 10 Measurements are obtained, and median stiffness is calculated	Widely available Rapid Repeatable	Operator dependent Not reliable in obese or hepatic steatosis No structural evaluation Confounders of increased liver stiffness
SWE	US transducer both generates and measures the shear waves Point SWE or 2D SWE Shear stiffness measured at variable frequencies	Can be combined with conventional US Structure visualization Real time stiffness measurements	Operator dependent Less accurate for mild fibrosis Confounders of increased stiffness
MR elastography	Most accurate method Performed at 60 Hz Same technique across all vendors and MR field strength Shear stiffness of liver is evaluated	High accuracy and diagnostic performance Easily performed with routine liver MRI study Not affected by steatosis	Requires additional dedicated hardware and software Severe iron overload may result in failure Confounders of increased stiffness

CT, computed tomography; MRI, magnetic resonance imaging; HCC, hepatocellular carcinoma; VCTE, vibration-controlled transient elastography; SWE, shear wave elastography; US, ultrasound; MR, magnetic resonance; MRI, magnetic resonance imaging.

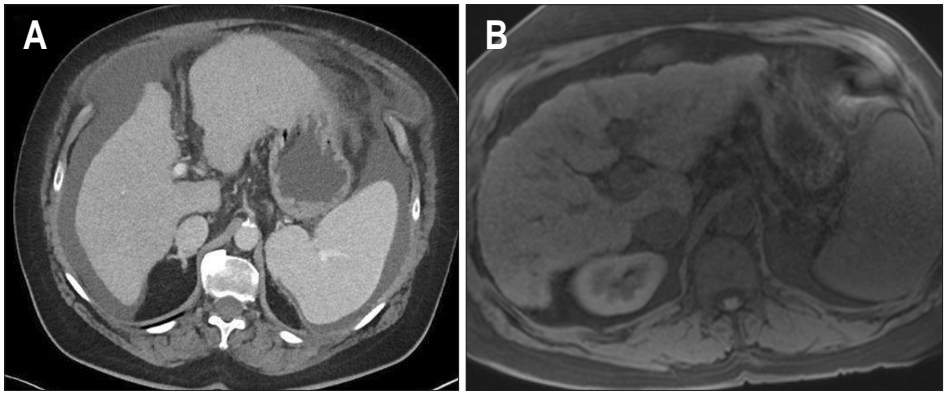

Fig. 8. Morphological changes of cirrhosis. Axial computed tomography (A) and T1W fat saturated (B) images (from two different patients) show morphological changes associated with cirrhosis including nodular liver margins, left lobe hypertrophy, fissure widening and prominence of fat at the hepatic hilum.

3. MR elastography

Currently, MRE is the most accurate noninvasive method for quantifying liver fibrosis and has gained acceptance as an alternative to liver biopsy.[31] The technique of MRE is a simple software and hardware addon and is available with both 1.5T and 3T MR scanners and can be easily incorporated into routine liver MR protocols. This technique involves transmitting shear waves through the liver to measure liver stiffness. It was first introduced in 2007 and Food and Drug Administration approved in 2009. The hardware includes an active driver outside the scanner room connected to a passive driver placed on the patient's midclavicular line, positioned over the right lobe of the liver.

During MRE, the passive driver vibrates at a fixed 60 Hz frequency and transmits shear waves throughout the liver. The tissue stiffness is directly proportional to the velocity of the shear wave, with cirrhotic liver tissue being stiffer than normal liver tissue, resulting in faster wave propagation. The MRE sequence captures this wave propagation, generating magnitude and phase images. The magnitude and phase images are processed using a wave inversion algorithm to produce stiffness maps.[32]

Typically, a gray scale elastogram map, a color elastogram map and a wave image are obtained (Figs 9 and 10). The ROI measurements is made on gray scale elastogram maps using either manual or automated methods to measure liver stiffness in kilopascals. Measurements should be obtained from at least four slices, and the mean stiffness value is calculated. The color elastogram map provides a qualitative assessment of stiffness with blue and purple indicating low stiffness and orange and red indicating higher stiffness. Care should be taken to avoid large vessels, fissures, the gallbladder, liver margins, and any liver masses

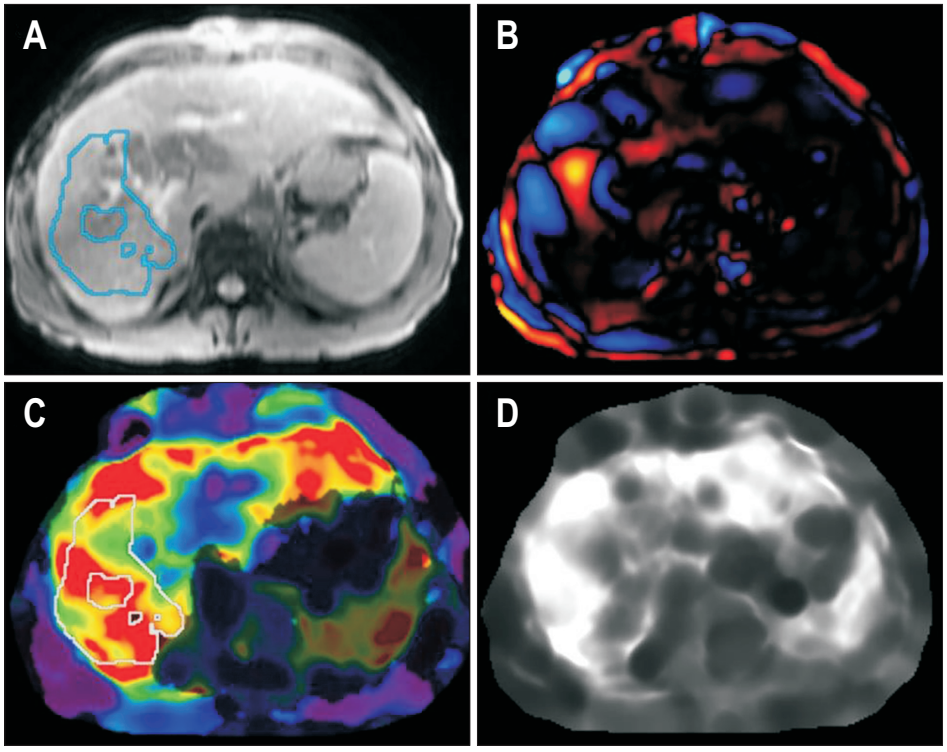

Fig. 9. Magnetic resonance elastogram in a patient with primary sclerosing cholangitis. Magnitude image (A), wave image (B), color elastogram (C) with the 95% confidence map (dark shaded areas) superimposed, and gray scale elastogram (D) are shown. The liver stiffness was 6.3 kPa, which is consistent with stage 4 fibrosis or cirrhosis.

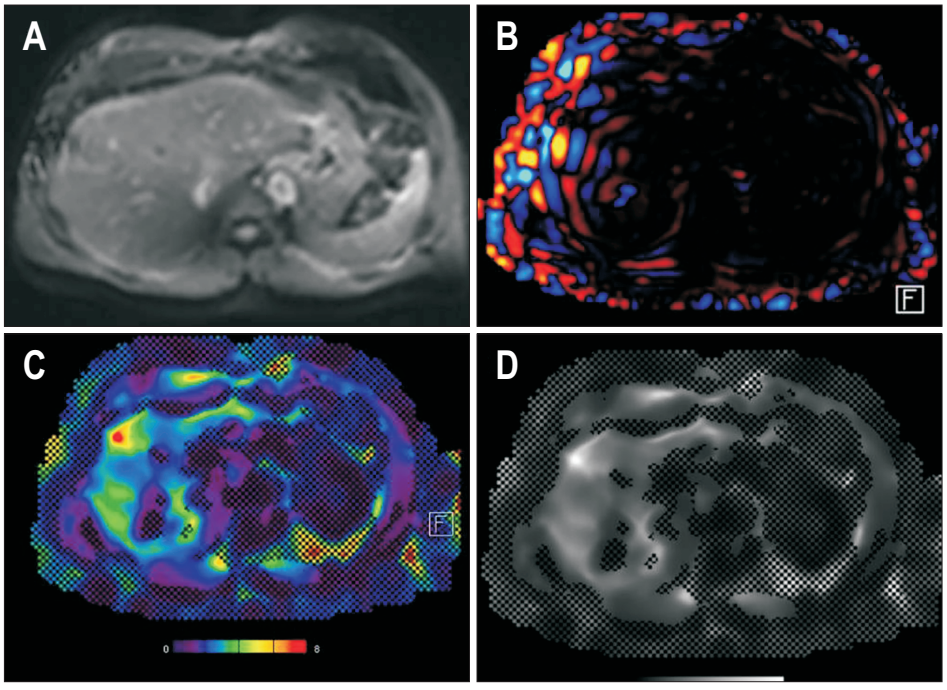

Fig. 10. Magnetic resonance elastogram of a patient with metabolic dysfunction-associated steatohepatitis. Magnitude image (A), wave image (B), color elastogram (C) and gray scale elastogram (D) are shown with the 95% confidence map (hatched out areas) superimposed. The liver stiffness was 3.1 kPa, which is consistent with stage 1–2 fibrosis.

during ROI selection to ensure accurate stiffness measurements. Intravenous MR contrast does not affect stiffness measurements, so MRE sequence can be added before or after contrast administration.

Liver stiffness calculated by MRE increases proportionally with the grade of fibrosis observed on histopathology, making it useful for assessing treatment response and disease progression (Table 5).[33] Additionally, MRE-derived stiffness values predict clinical outcomes including decompensation of the liver disease and death.[34] A stiffness value of >3.5 kPa is usually considered as significant fibrosis (F2 disease).

One major advantage of MRE is its ability to evaluate the entire cross-section of the liver. Liver fibrosis can vary

across lobes and segments, and MRE mitigates the sampling errors associated with vibration-controlled transient elastography and liver biopsy. MRE also performs well in patients with ascites and obesity. However, limitations include limited availability and cost.

An important cause of low-quality MRE study is technical failure due to susceptibility artifacts from iron overload in the liver or other paramagnetic materials like embolization coils, transjugular intrahepatic portosystemic shunt in the scan volume.[35] It is also important to consider that factors other than fibrosis can elevate liver stiffness, such as the post-prandial state, acute hepatitis, passive hepatic congestion, infiltrative disease, and cholestasis.[31] These confounders can falsely elevate liver stiffness across all elastography techniques including MRE, US-based transient elastography, and shear wave elastography. Therefore, stiffness values should be interpreted in the context of the patient's clinical presentation. Additionally, patients should fast for at least 3 to 4 hours prior to the procedure to optimize MRE accuracy. Other newer CT and MR techniques in liver fibrosis assessment are briefly described in Table 6. However, these techniques are still under evaluation or not widely available for clinical use. Further clinical experience in these techniques is awaited before their application.

Table 5. Liver Stiffness Measurement with MR Elastography and Corresponding Fibrosis Stages

MR liver stiffness	Fibrosis stage
<2.5 kPa	Normal
2.5 to <3.0 kPa	Normal or inflammation
3.0 to <3.5 kPa	Stage 1–2 fibrosis
3.5 to <4.0 kPa	Stage 2–3 fibrosis
4.0 to <5.0 kPa	Stage 3–4 fibrosis
>5.0 kPa	Stage 4 fibrosis or cirrhosis

MR, magnetic resonance.

CONCLUSION

In conclusion, imaging modalities, particularly MRI with CSE sequences and MRE, play a crucial role in the comprehensive evaluation and management of CLD. Confounder-corrected CSE MRI can simultaneously measure liver fat (PDFF) and iron (R2*) with accuracy comparable to biopsy, while MRE is the best imaging technique currently available to measure liver stiffness. These noninvasive quantitative imaging biomarkers have emerged as a viable alternative to liver biopsy in many clinical scenarios. While MRI remains a cornerstone in this domain, CT and US offer complementary roles due to their broader availability and reduced cost. Continued advancements

Table 6. Emerging CT and MRI Techniques for Evaluating Liver Fibrosis

Technique	Description	Current role
Dual-energy CT	Iodine concentration (on 5 min delayed images) has been shown to correlate with fibrosis stage on histology	Limited role Investigational technique Not useful in early fibrosis
HBA and collagen targeted contrast agents	The uptake of HBA by the hepatocytes decreases with increasing fibrosis. The post HBA images can be compared with precontrast images to detect the stage of fibrosis Recently introduced collagen targeted MRI contrast agents have shown promise in detection early fibrosis in *in vitro* studies	Promising Investigational
T1 mapping	Liver fibrosis results in expansion of ECV T1 mapping can calculate ECV and is shown to correlate with fibrosis	Lower diagnostic performance Probable role where other MR techniques are not available
T2 mapping	Increased T2 values indicate edema/ inflammation and can correlate with fibrosis Has also been shown to be useful in quantification of hepatic steatosis	Investigational technique
Diffusion weighted imaging	Fibrosis limits the movement of water molecules resulting in increased diffusion restriction and low apparent diffusion coefficient values	Lower accuracy compared to MR elastography Susceptibility to motion artifacts Not reproducible across scanners and vendors
Spin-lattice relaxation	Measures T1 relaxation Fibrotic areas exhibit altered T1 relaxation times compared to normal liver	Investigational/research technique

CT, computed tomography; MRI, magnetic resonance imaging; HBA, hepatobiliary contrast agent; ECV, extracellular volume; MR, magnetic resonance.

in imaging technology promise to further refine our understanding and management of CLD, improving patient outcomes and quality of care.

CONFLICTS OF INTEREST

Mayo Clinic and the author M.Y. have intellectual properties that associated with magnetic resonance imaging elastography. Except for that, no potential conflict of interest relevant to this article was reported.

AUTHOR CONTRIBUTIONS

Drafting of the manuscript: S.N., M.Y., M.F., I.S.I. Revision of the manuscript for important intellectual content S.K.V. Approval of final manuscript: all authors.

ORCID

Sabarish Narayanasamy https://orcid.org/0000-0002-6649-327X
Manuela Franca https://orcid.org/0000-0003-1068-8577
Ilkay S. Idilman https://orcid.org/0000-0002-1913-2404
Meng Yin https://orcid.org/0000-0001-6778-192X
Sudhakar K. Venkatesh https://orcid.org/0000-0002-7514-1030

REFERENCES

1. Younossi ZM, Koenig AB, Abdelatif D, Fazel Y, Henry L, Wymer M. Global epidemiology of nonalcoholic fatty liver disease: meta-analytic assessment of prevalence, incidence, and outcomes. Hepatology 2016;64:73-84.
2. Rinella ME, Lazarus JV, Ratziu V, et al. A multisociety Delphi consensus statement on new fatty liver disease nomenclature. Hepatology 2023;78:1966-1986.
3. Kalisz K, Navin PJ, Itani M, Agarwal AK, Venkatesh SK, Rajiah PS. Multimodality imaging in metabolic syndrome: state-of-the-art review. Radiographics 2024;44:e230083.
4. Issa R, Williams E, Trim N, et al. Apoptosis of hepatic stellate cells: involvement in resolution of biliary fibrosis and regulation by soluble growth factors. Gut 2001;48:548-557.
5. Ganz M, Bukong TN, Csak T, et al. Progression of non-alcoholic steatosis to steatohepatitis and fibrosis parallels cumulative accumulation of danger signals that promote inflammation and liver tumors in a high fat-cholesterol-sugar diet model in mice. J Transl Med 2015;13:193.
6. Arab JP, Barrera F, Arrese M. The evolving role of liver biopsy in non-alcoholic fatty liver disease. Ann Hepatol 2018;17:899-902.
7. Ferraioli G, Soares Monteiro LB. Ultrasound-based techniques for the diagnosis of liver steatosis. World J Gastroenterol 2019;25:6053-6062.
8. Zhang YN, Fowler KJ, Hamilton G, et al. Liver fat imaging-a clinical overview of ultrasound, CT, and MR imaging. Br J Radiol 2018;91:20170959.
9. Ozturk A, Kumar V, Pierce TT, et al. The future is beyond bright: the evolving role of quantitative US for fatty liver disease. Radiology 2023;309:e223146.
10. Pickhardt PJ, Graffy PM, Reeder SB, Hernando D, Li K. Quantification of liver fat content with unenhanced MDCT: phantom and clinical correlation with MRI proton density fat fraction. AJR Am J Roentgenol 2018;211:W151-W157.
11. Pickhardt PJ, Park SH, Hahn L, Lee SG, Bae KT, Yu ES. Specificity of unenhanced CT for non-invasive diagnosis of hepatic steatosis: implications for the investigation of the natural history of incidental steatosis. Eur Radiol 2012;22:1075-1082.
12. Starekova J, Hernando D, Pickhardt PJ, Reeder SB. Quantification of liver fat content with CT and MRI: state of the art. Radiology 2021;301:250-262.
13. Reeder SB, Cruite I, Hamilton G, Sirlin CB. Quantitative assessment of liver fat with magnetic resonance imaging and spectroscopy. J Magn Reson Imaging 2011;34:729-749.
14. Colgan TJ, Zhao R, Roberts NT, Hernando D, Reeder SB. Limits of fat quantification in the presence of iron overload. J Magn Reson Imaging 2021;54:1166-1174.
15. Idilman IS, Keskin O, Celik A, et al. A comparison of liver fat content as determined by magnetic resonance imaging-proton density fat fraction and MRS versus liver histology in non-alcoholic fatty liver disease. Acta Radiol 2016;57:271-278.
16. Pooler BD, Hernando D, Reeder SB. Clinical implementation of a focused MRI protocol for hepatic fat and iron quantification. AJR Am J Roentgenol 2019;213:90-95.
17. Labranche R, Gilbert G, Cerny M, et al. Liver iron quantification with MR imaging: a primer for radiologists. Radiographics 2018;38:392-412.
18. Valenti L, Corradini E, Adams LA, et al. Consensus statement on the definition and classification of metabolic hyperferritinaemia. Nat Rev Endocrinol 2023;19:299-310.
19. Gandon Y, Olivié D, Guyader D, et al. Non-invasive assessment of hepatic iron stores by MRI. Lancet 2004;363:357-362.
20. Boll DT, Merkle EM. Diffuse liver disease: strategies for hepatic CT and MR imaging. Radiographics 2009;29:1591-1614.
21. Welle CL, Olson MC, Reeder SB, Venkatesh SK. Magnetic

resonance imaging of liver fibrosis, fat, and iron. Radiol Clin North Am 2022;60:705-716.
22. Reeder SB, Yokoo T, França M, et al. Quantification of liver iron overload with MRI: review and guidelines from the ESGAR and SAR. Radiology 2023;307:e221856.
23. Sirlin CB, Reeder SB. Magnetic resonance imaging quantification of liver iron. Magn Reson Imaging Clin N Am 2010;18:359-381.
24. St Pierre TG, Clark PR, Chua-Anusorn W. Single spin-echo proton transverse relaxometry of iron-loaded liver. NMR Biomed 2004;17:446-458.
25. Hankins JS, McCarville MB, Loeffler RB, et al. R2* magnetic resonance imaging of the liver in patients with iron overload. Blood 2009;113:4853-4855.
26. Marrero JA, Kulik LM, Sirlin CB, et al. Diagnosis, staging, and management of hepatocellular carcinoma: 2018 practice guidance by the American Association for the Study of Liver Diseases. Hepatology 2018;68:723-750.
27. Barr RG, Wilson SR, Rubens D, Garcia-Tsao G, Ferraioli G. Update to the Society of Radiologists in Ultrasound liver elastography consensus statement. Radiology 2020;296:263-274.
28. Mamone G, Cortis K, Sarah A, Caruso S, Miraglia R. Hepatic morphology abnormalities: beyond cirrhosis. Abdom Radiol (NY) 2018;43:1612-1626.
29. Ozaki K, Matsui O, Kobayashi S, Minami T, Kitao A, Gabata T. Morphometric changes in liver cirrhosis: aetiological differences correlated with progression. Br J Radiol 2016;89:20150896.
30. Ludwig DR, Fraum TJ, Ballard DH, Narra VR, Shetty AS. Imaging biomarkers of hepatic fibrosis: reliability and accuracy of hepatic periportal space widening and other morphologic features on MRI. AJR Am J Roentgenol 2021;216:1229-1239.
31. Moura Cunha G, Fan B, Navin PJ, et al. Interpretation, reporting, and clinical applications of liver MR elastography. Radiology 2024;310:e231220.
32. Guglielmo FF, Venkatesh SK, Mitchell DG. Liver MR elastography technique and image interpretation: pearls and pitfalls. Radiographics 2019;39:1983-2002.
33. Huwart L, Sempoux C, Vicaut E, et al. Magnetic resonance elastography for the noninvasive staging of liver fibrosis. Gastroenterology 2008;135:32-40.
34. Gidener T, Yin M, Dierkhising RA, Allen AM, Ehman RL, Venkatesh SK. Magnetic resonance elastography for prediction of long-term progression and outcome in chronic liver disease: a retrospective study. Hepatology 2022;75:379-390.
35. Ghoz HM, Kröner PT, Stancampiano FF, et al. Hepatic iron overload identified by magnetic resonance imaging-based T2* is a predictor of non-diagnostic elastography. Quant Imaging Med Surg 2019;9:921-927.